Ice thickness, areal and volumetric changes of Davies Dome and Whisky Glacier (James Ross Island, Antarctic Peninsula) in 1979–2006

Zbyněk ENGEL,[1,2] Daniel NÝVLT,[2] Kamil LÁSKA[3]

[1]Department of Physical Geography and Geoecology, Charles University in Prague, Praha, Czech Republic
E-mail: engel@natur.cuni.cz
[2]Czech Geological Survey, Brno, Czech Republic
[3]Department of Geography, Masaryk University, Brno, Czech Republic

ABSTRACT. This study calculates area, volume and elevation changes of two glaciers on James Ross Island, Antarctica, during the period 1979–2006. Davies Dome is a small ice cap. Whisky Glacier is a valley glacier. Ground-penetrating radar surveys indicate ice thickness, which was used for calculations of the bed topography and volume of both glaciers. Maximum measured ice thicknesses of Davies Dome and Whisky Glacier are 83 ± 2 and 157 ± 2 m, respectively. Between 1979 and 2006, the area of the ice cap decreased from 6.23 ± 0.05 km^2 to 4.94 ± 0.01 km^2 (–20.7%), while the area of the valley glacier reduced from 2.69 ± 0.02 km^2 to 2.40 ± 0.01 km^2 (–10.6%). Over the same period the volume of the ice cap and valley glacier reduced from 0.23 ± 0.03 km^3 to 0.16 ± 0.02 km^3 (–30.4%) and from 0.27 ± 0.02 km^3 to 0.24 ± 0.01 km^3 (–10.6%), respectively. The mean surface elevation decreased by 8.5 ± 2.8 and 10.1 ± 2.8 m. The average areal ($\sim$0.048–0.011 km^2 a^{-1}) and volumetric ($\sim$0.003–0.001 km^3 a^{-1}) changes are higher than the majority of other estimates from Antarctic Peninsula glaciers.

INTRODUCTION

The mean annual temperature in the Antarctic Peninsula (AP) region has increased by 1.5°C to 3.0°C since the 1950s (e.g. King, 1994; Vaughan and others, 2001, 2003; Turner and others, 2005). This warming has coincided with the disintegration of ice shelves and the retreat of many land-terminating glaciers in the region (e.g. Skvarca and others, 1998; Cook and others, 2005; Davies and others, 2011; Glasser and others, 2011). Land-based glacial mass loss has been most prominent at the northern tip of the AP due to the pronounced glacier acceleration (Rignot and others, 2008). Detailed analyses of satellite imagery and some isolated mass-balance measurements together suggest that small land-terminating glaciers are especially sensitive to climate change (Rau and others, 2004; Skvarca and others, 2004). The sensitivity of small land-terminating glaciers to climate is related to a short response time of variations in mass balance (Knap and others, 1996).

Along with direct mass-balance measurements, changes in surface area and volume of glaciers are important indicators of climate changes. Volumetric characteristics are necessary for improved understanding of: (1) the responses of these sensitive glacier systems to climate change; (2) the present contribution of AP glaciers to sea-level rise; and (3) future predictions of AP glacier behaviour. Although changes in glacier mass over long time periods can be analysed by volumetric methods, these do not replace the field-based techniques, which provide detailed measures of glacier change in space and time. Direct methods are time-consuming and expensive, however, and typically only cover short time periods (Gudmundsson and Bauder, 1999). Glacier bed topography and ice thickness are important for understanding ice dynamics (e.g. Rippin and others, 2011a) and for assessing basal pressure and thermal regimes (e.g. Rippin and others, 2011b). Determination of glacial mass changes may be used to detect shifts in climate and to

predict glacial changes associated with future climate conditions (e.g. Paterson, 1994; Fountain and others, 1999).

In this study, we present the volumetric data for Davies Dome ice cap and Whisky Glacier on James Ross Island (JRI). The name Whisky Glacier is used here for IJR-45 glacier as given in the inventory by Rabassa and others (1982). The name Whisky Glacier was referred to by Chinn and Dillon (1987) and is given on the Czech Geological Survey (2009) map. It should not be confused with the tidewater Whisky Glacier located in Whisky Bay, as named by the British Antarctic Survey (2010). The changes in elevation, area and geometry between 1979 and 2006 were derived from digital elevation models (DEMs) and aerial photographs. Ice thickness was measured during a field campaign in January and February 2010 using ground-penetrating radar (GPR). Glacier volume and glacier bed elevations were then derived from these data.

STUDY AREA

Approximately 81% of JRI is covered with 138 glaciers, which are concentrated in the central and southern parts of the island (Rabassa and others, 1982). The variety of existing glacier systems and fluctuations of glacier front positions on JRI have been presented by Rabassa and others (1982), Skvarca and others (1995) and Rau and others (2004). Mass-balance changes have been studied at Glaciar Bahía del Diablo on Vega Island (Skvarca and others, 2004) and at Davies Dome and Whisky Glacier on JRI (Nývlt and others, 2010; Láska and others, 2012). However, these existing glaciological studies only describe elevation and surface area; data on ice thickness and hence on ice volume are hitherto unknown.

The investigated glaciers are located on the Ulu Peninsula, northern JRI (Fig. 1). This predominantly glacier-free area extends northwards from the central part

of the island, which is dominated by the JRI ice field, an area of ice covering 587 km^2 (Rabassa and others, 1982). The climate of the Ulu Peninsula is influenced by the regional-scale atmospheric circulation formed by the AP, which generally provides a barrier to westerly winds associated with cyclonic systems centred in the circumpolar trough (King and others, 2003). High interdiurnal and seasonal variability of cloudiness, incoming solar radiation and near-surface air temperature can be found along the eastern coast of the AP (Marshall, 2002; Láska and others, 2011) although the long-term trend appears to involve increased frequency of warm airflows advected over the AP as described by Marshall and others (2006).

Contemporary glaciation of JRI is characterized by ice caps, outlet glaciers and different types of alpine glaciers (Rabassa and others, 1982). The JRI ice field covers the southern part of the island where only small masses of rock protrude to the surface. By contrast, most ice has retreated from the northern part of the Ulu Peninsula. Small glaciers have persisted in higher locations with snow accumulation areas above ~460 m a.s.l. (Nývlt and others, 2010). The glacial features include an ice cap on Davies Dome (514 m) and on Lachman Crags (641 m), cirque, apron and piedmont glaciers around these plateaux, and valley glaciers carved into Smellie Peak (704 m) and Stickle Ridge (767 m). These glaciers are relics of an ice cap that covered the whole island in the last glacial period (Rabassa, 1983; Ingólfsson and others, 1992). In the northern part of JRI, this ice cap merged with the northern Prince Gustav Ice Stream, which drained the northeastern AP (Rabassa, 1983). During the Holocene, the ice cap was linked to the Röhss Bay Ice Shelf, until it disintegrated in 1995 (Glasser and others, 2011).

Two contrasting types of glacier from the Ulu Peninsula were selected to assess recent volume changes. Davies Dome (DD) is an ice dome (63°52′–63°54′ S, 58°01–58°06′ W) which originates on the surface of a flat volcanic mesa at >400 m a.s.l. and terminates as a single 700 m wide outlet in Whisky Bay. In 2006, DD had an area of ~6.5 km^2 and lay in the altitude range 0–514 m a.s.l. (Table 1). Whisky Glacier (WG) is a cold-based land-terminating valley glacier (63°55′–63°57′ S, 57°56′–57°58′ W), which is surrounded by an extensive area of debris-covered ice (Chinn and Dillon, 1987). In 2006, the glacier covered an area of ~2.4 km^2 and ranged from 520 to 215 m a.s.l. Mean annual near-surface air temperatures of –7.8°C and –8.8°C have been recorded since 2009 by automatic weather stations (AWSs) on WG (356 m) and DD (514 m), respectively (Fig. 1). Summer temperatures (November–February) vary from –9°C to +10°C on WG and from –12°C to +7°C on DD. The snowmelt period generally starts at the beginning of November and lasts until the end of February. The meteorological data were collected as part of this study using AWSs on glaciers (Fig. 1).

DATA AND METHODS

DEMs and aerial photographs of DD and WG were used to extract topographic information for glacier extent and geometry. Two separate DEMs produced by the GEODIS company (Czech Republic) were stereoplotted from aerial photographs obtained by the British Antarctic Survey (BAS) in 1979 and 2006 (Czech Geological Survey, 2009). Ground-control points for the photogrammetric processing were obtained in the deglaciated landscape in 2008 using a dual-frequency differential GPS receiver. The 1979 aerial
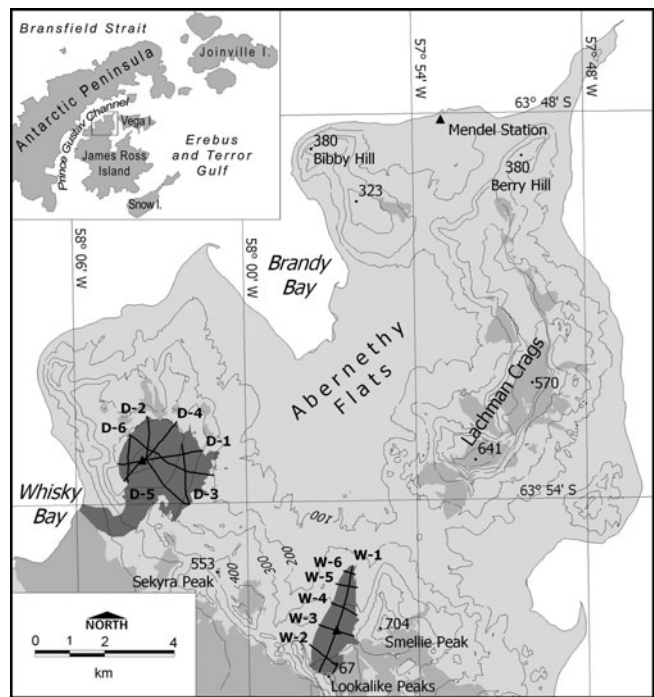

Fig. 1. Location of GPR transects (labelled as D-*n* and W-*n*, *n* being an integer) on Davies Dome and Whisky Glacier (dark grey areas) on the Ulu Peninsula, northern JRI. Other ice bodies are shown in medium grey. Triangles mark the position of meteorological stations.

photos were registered with root-mean-square (rms) errors of 2.0 m in both the horizontal and vertical. Rms errors of the 2006 dataset are 0.7 m and 0.8 m in the horizontal and vertical direction, respectively. Meixner (2009) provides a more complete description of the DEM generation method.

The GPR survey was conducted in January and February 2010 in accordance with numerous descriptions of radar investigations of glacier thickness (e.g. Plewes and Hubbard, 2001; Navarro and Eisen, 2010). GPR surveys were applied on DD (except over a steep and crevassed outlet glacier) and across the whole surface of WG. GPR data were collected along six radial profiles on DD (Fig. 1). On WG, GPR was carried out along the central longitudinal profile and five transverse profiles (Fig. 1). A longitudinal profiling was carried out from the glacier terminus to the upper reaches of the ablation zone (226–444 m a.s.l.). Three transverse profiles were undertaken in the lower part of the snout delimited by lateral moraines and two profiles in the upper zone enclosed by the left lateral moraine and a valley slope facing to the west. GPR profiling was carried out using an unshielded 50 MHz Rough Terrain Antenna and RAMAC CU-II control unit (MALÅ GeoScience, 2005). The signal acquisition time was set to 2040 ns, and scan spacing ranged from 0.2 to 0.3 m. GPR position was given by GPS: a Garmin GPSMAP 60CSx receiver (Garmin International, 2009) was used to determine coordinates for the corresponding trace numbers with the horizontal rms position accuracy <4 m. The GPR profiling equipment was man-hauled at a mean speed of ~0.5 m s^{-1}.

GPR data were processed and interpreted using the REFLEXW software version 5.0 (Sandmeier, 2008). The raw GPR profiles were filtered using an automatic gain function (AGC-Gain), background removal and static correction. The AGC-Gain was used to amplify deep signals reduced due to pulse dispersion and attenuation. Strong direct wave signal

Table 1. Morphological characteristics of DD and WG for 2006

Name	Type	Elevation range	Mean elevation	Mean thickness	Maximum thickness	Length*	Area	Volume
		m a.s.l.	m a.s.l.	m	m	km	km^2	km^3
Davies Dome	Dome	124–515	368.5 ± 0.8	32.4 ± 1.2	83 ± 2	3.43[†]	4.94 ± 0.01	0.16 ± 0.02
							6.49 ± 0.01[†]	
Whisky Glacier	Valley	215–520	340.6 ± 0.8	99.6 ± 1.8	158 ± 2	3.19	2.40 ± 0.01	0.24 ± 0.01

*The length was measured along the central axis of the DD outlet and WG snout.
[†]The value for the whole of DD including the outlet glacier.

and noise reflections were eliminated using the background removal filter. Finally, the radargrams were corrected for topographic elevation. For this purpose, elevations from the collected GPS data were used. Depth was calculated assuming a wave velocity for cold glacier ice, 0.168 m ns^{-1} (Narod and Clarke, 1994). The velocity model used to convert two-way travel times to depths affects the accuracy of the ice thickness determination. As signal velocities in glacier ice range from 0.167 to 0.169 m ns^{-1} (Kovacs and others, 1995; Pellikka and Rees, 2009), the velocity used was accurate to within 0.002 m ns^{-1}. Thus, the estimated uncertainty of conversion of travel time to depth is ~1%. Moreover, the accuracy in depth measurement is restricted by the ability to determine the first arrival of the signal (Jol, 2009). This uncertainty was approximated by a quarter of the signal's wavelength in ice, which corresponds to 0.84 m for the 50 MHz antenna used.

Ice-thickness values converted from two-way travel times along GPR profiles were used to calculate glacier volumes. Because the accuracy of the calculation depends on the algorithm applied we investigated and selected the most appropriate interpolation first. We applied five techniques (inverse distance weighing, kriging, minimum curvature, spatial neighbour and triangulation) to the complete ice-thickness datasets to create grids of glaciers. We then removed the ice-thickness information along one complete section from each of the two datasets. We selected the section D-1, which represents both the upper part of an ice dome on a flat volcanic plateau and the lower termination on mountain slopes. For WG, we chose the section W-4 as it crosses the middle part of the snout. The reduced datasets and the same interpolation techniques were used to generate a new series of grids from which ice-thickness values were assigned for verification points along sections D-1 and W-4. The interpolated values were compared with the measured values and the difference was expressed using standard deviation values. Results of interpolation techniques were also evaluated based on glacier volumes calculated from a complete and reduced dataset. A comparison of the calculated values shows that the minimum curvature technique most accurately represents the ice-thickness data (Table 2). This method was selected for further processing of the data.

The volume of glaciers was calculated using a combination of 2006 surface elevation data and GPR-based ice-thickness data taken in 2010. The elevation of GPS-derived locations along GPR profiles was taken from the 2006 DEM because the accuracy of an altitude measurement was low during the GPR survey. The vertical error of GPS-based coordinates (~8–18 m) is larger than the vertical error of the DEM and elevation changes of glacier surfaces between

2006 and 2010. According to mass-balance measurements on DD and WG the elevation differences ranged from –0.4 to +1.1 m during this period (Nývlt and others, 2012). The volume of glaciers for 1979 was calculated based on the 2006 volumes and the difference between 1979 and 2006 surface DEMs. The uncertainty associated with the glacier volume determination was calculated as the product of the glacier surface area and vertical uncertainty. The vertical uncertainty for 2006 is related to the accuracy of ice thickness and to surface elevation changes in 2006–10. The uncertainty for 1979 was calculated as the sum of the glacier surface topography-related uncertainty for 1979 plus the uncertainty of the glacier volume for 2006. The mean ice thickness of DD and WG is 32.4 and 99.6 m, respectively, and average uncertainties of conversion of travel time to ice thickness are 0.3 and 1.0 m, respectively. The total uncertainty of the ice volume per glacier area in 2006 is 3.5 m^3 m^{-2} for DD and 4.1 m^3 m^{-2} for WG. Uncertainties of 5.5 and 6.1 m^3 m^{-2} have been obtained for the 1979 volume of DD and WG, respectively.

Glacier bed topography maps were generated based on the 2006 DEM and the 2010 GPR measurements. The bed elevation was calculated for GPR survey locations by subtracting the ice thickness from the surface elevation. At the margin of DD, the ice thickness was set to zero except for the upper reaches for the outlet where three bounding points were placed. For these points, depth values were approximated from the nearest points of GPR measurements and from the position of a small rock outcrop that protrudes to the surface of the eastern part of the outlet. The bed elevation at the WG limit was determined from marginal measurement points at GPR cross-sections that represent the crest of lateral moraines. The minimum curvature interpolation, which generates a smoothed surface with low standard deviation, was then used to construct an 8 m gridcell DEM of glacier beds. From the DEMs, contour lines at 10 m spacing were constructed for bed topography.

RESULTS

Glacier bed topography

The boundary between the glaciers and underlying bedrock and/or till is recorded as continuous basal reflection in all of our radargrams (Figs 2 and 3). A strong reflection at the glacier bed is clearly visible in DD profiles where the slope of the presumed bedrock is small (Fig. 2a and c). By contrast, the amplitude of reflections is halved in the area below the subglacial eastern flank of the plateau as shown in transect D-3 (Fig. 2b) and in the eastern sections of transects D-1,

Table 2. Results of glacier volume calculations

Gridding method	Davies Dome			Whisky Glacier		
	Volume	SD*	$\Delta V^{\dagger}$	Volume	SD*	$\Delta V^{\dagger}$
	km³		%	km³		%
Inverse distance weighing	0.153	10.2	2.0	0.236	33.8	0.5
Kriging	0.153	10.5	1.9	0.236	33.5	0.6
Minimum curvature	0.160	8.5	1.1	0.239	21.0	0.2
Spatial neighbour	0.152	10.7	2.3	0.232	29.7	0.6
Triangulation	0.154	9.4	2.4	0.232	20.7	0.5

*Standard deviation of interpolated ice thickness along sections D-1 and W-4.
†Difference in glacier volume interpolated based on complete dataset and on data without sections D-1 and W-4.

D-2 and D-6. Beneath WG, the strong and continuous reflection was recorded in the upper half of profile W-1 (Fig. 3a). There are only a few minor diffractions visible along the glacier bed in this section. The signal strength decreases slightly in the middle section of the longitudinal profile ~1.8 km from the glacier terminus. The decreased amplitude prevails in the lower part of the snout as seen along the lower part of the longitudinal profile and in cross-profiles W-4, W-5 and W-6 (Fig. 3c).

The subglacial topography of DD is relatively complex. The uppermost part of DD is located on a near-horizontal surface. GPR data indicate a slightly undulating glacier bed with an elevation range of <50 m (Fig. 2a and c). Most of the near-flat bed is inclined to the north, and only ~7% of this zone faces southeast or south. An undulating glacier bed extends to half the length of the northwest–southeast axis of DD. Here the reflection boundary descends from 400–430 m a.s.l. by 70–90 m to more dissected bed topography (Fig. 2b). The fall line is oriented towards the southeast and represents an eastern flank of the volcanic plateau (Fig. 4a). Steeper slopes and concave wide channel-like depressions are indicated in the radargrams of two sections of the flank.

The southernmost of these coincides with the main outlet glacier that drains DD into Whisky Bay. The second slope depression is carved into the central part of the bedrock step ~1 km from DD summit to the east.

WG bed interface has a simple geometry. The data obtained along the centre flowline show an even longitudinal profile without any subglacial steps or depressions (Fig. 3a). The bed topography is inclined to the north with low average slope angle of ~5°. The mean slope of the basal contact in the lower part of the profile is <2°. The transverse profiles W-2 and W-3 across the central line of WG show an asymmetric bottom of a trough with steeper slopes rising towards the east, where the glacier is constricted by a steep slope of Smellie Peak (Fig. 3b). The western part of the bed topography is characterized by a gentle slope angle, which is within 5° of the glacier surface. As a result, the glacier bed is located up to ~125 m below the western margin of the glacier surface (Fig. 5). The pattern of the bed topography suggests that ice extends as a debris-covered glacier towards the west. Similar conditions are recorded in transverse profiles W-4, W-5 and W-6, which were undertaken in the lower part of WG. These
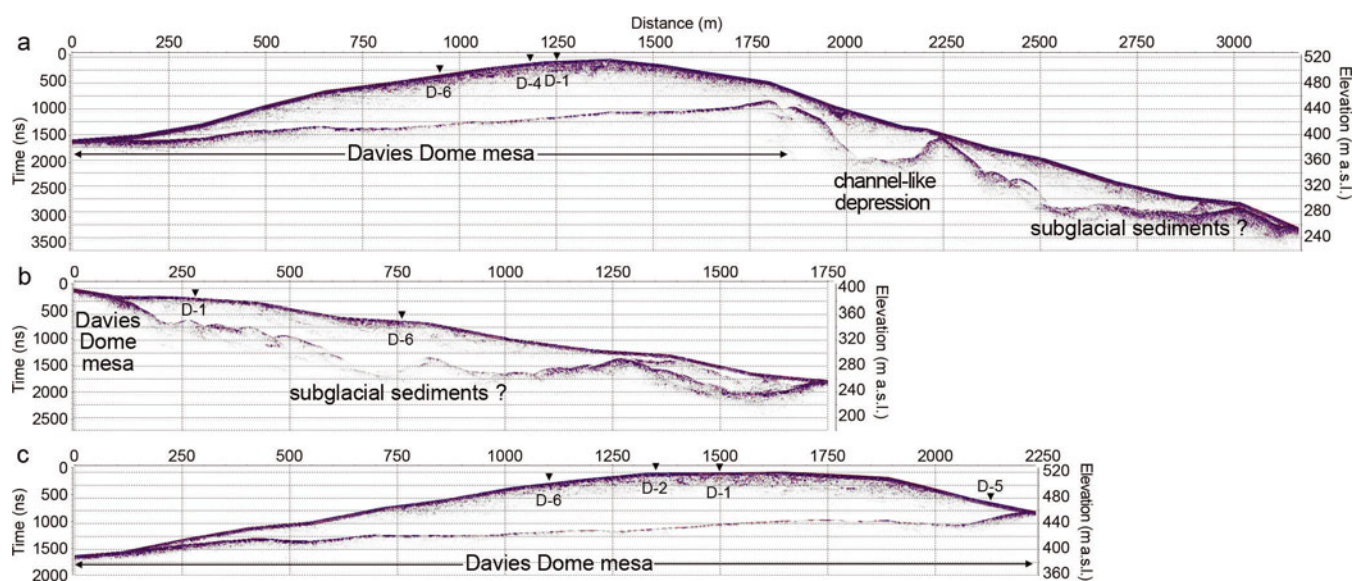

Fig. 2. Selected GPR transects across DD. (a) Profile D-2 covers the dome glacier in the northwest–southeast direction showing the subglacial surface of the DD mesa and its transition to more undulated bed topography in the eastern part of DD. (b) Profile D-3 shows the lower part of the glacier below the eastern margin of the DD mesa. (c) Profile D-4 shows the upper flat-bottomed part of the glacier. Inverted triangles indicate points of crossover of other profiles.
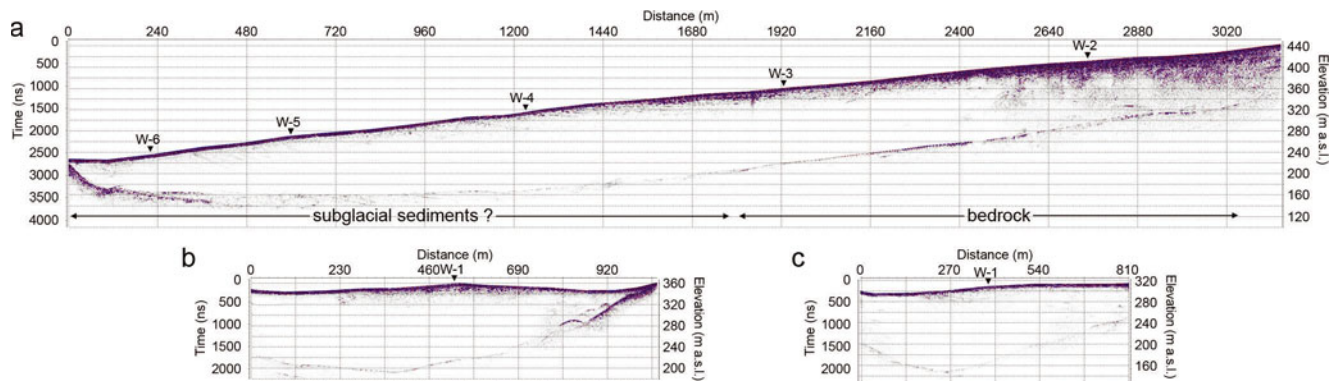
Fig. 3. Longitudinal transect W-1 (a) and cross-sectional transects W-3 (b) and W-4 (c) for WG. The position of the glacier bed along the western margin of WG indicates that glacier ice continues to the west (b, c). The ice thickness on the eastern side of profile W-4 suggests that the right lateral moraine delimiting the snout is also ice-cored (c). Inverted triangles indicate points of crossover of other profiles.

profiles suggest that the glacier ice also extends beyond the eastern margin of WG forming a core of a right lateral moraine (Fig. 3c). The minimum extent of debris-covered ice is $\sim$0.5 km^2. However, if the whole area of lateral and terminal moraines is taken into account then the maximum extent of ice-covered moraines is $\sim$3 km^2.

Surface area, elevation and volume change

The area of DD in 1979 was 8.33 ± 0.06 km^2 and in 2006 was 6.49 ± 0.01 km^2. The dome area decreased from 6.23 ± 0.05 to 4.94 ± 0.01 km^2, losing 20.7% of its area (Table 3). Assuming a constant rate of change, the ice cap therefore lost 0.048 ± 0.002 km^2 a^{-1}. Almost 70% of measured areal loss occurred in the southeast periphery of the dome at 120–370 m a.s.l.

Over the same time period, WG lost 10.6% of its non-debris-covered area, decreasing from 2.69 ± 0.02 km^2 to 2.40 ± 0.01 km^2. The mean glacier loss rate was 0.011 ± 0.001 km^2 a^{-1}. The form of WG remained almost the same during this period. In 1979 its terminus descended to 210 m a.s.l. and terminated behind a complex of

ice-cored terminal moraines. By 2006 the snout had retreated by $\sim$60 m, with a mean retreat rate of 2.2 m a^{-1} terminating at 215 m a.s.l.

DEM comparisons show surface elevation changes between 1979 and 2006 for each glacier. Surface lowering occurred over 95% of the surface of DD, which lowered on average by 8.5 ± 2.8 m. Most of the loss occurred in the southern and western part of the dome (Fig. 6). The site that experienced the greatest reduction in surface elevation ($\sim$35 $\pm$ 3 m) was occupied on 25 January 2010 by a supraglacial lake (our observation during GPR survey). Surface lowering greater than 25 m occurred on the whole southern part of the dome, where DD glacier descends over rugged relief at lower elevations (300–330 m a.s.l.). The dome glacier surface decreased by $\sim$20 $\pm$ 3 m around its western margin, which is located on Davies Mesa at 400–460 m a.s.l. The upper parts of the northwestern slope of the dome above 450 m a.s.l. experienced lesser changes in surface elevation (<10 m). The surface area located to the north from the highest part of the dome remained either unaltered or increased by <10 m.
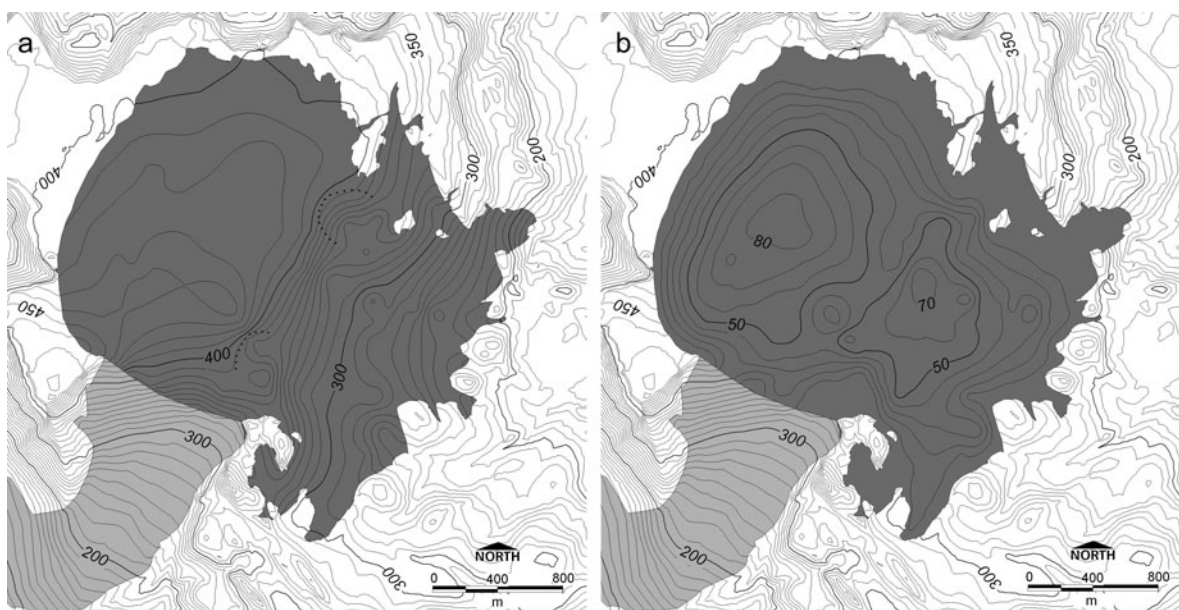

Fig. 4. (a) Glacier bed topography and (b) ice thickness at DD based on the 2006 DEM and GPR measurements. The investigated dome glacier is marked in dark grey and the outlet glacier is shown in medium grey.

Surface elevations of WG decreased on average by 10.1 ± 2.8 m over the period 1979–2006. The whole glacier experienced lowering, with the greatest reduction in surface elevations (>25 m) in the upper snow accumulation area (Fig. 7). On average, surface elevations of WG decreased at a rate of 0.37 ± 0.11 m a^{-1}. This value is slightly higher than the mean surface lowering for DD (0.32 ± 0.11 m a^{-1}).

GPR data obtained between 25 January and 17 February 2010 reveal the ice thickness of the two glaciers (Table 1; Figs 4b and 5b). At DD, the maximum thickness of 83 ± 2 m was recorded on its highest part near the crossing of the D-2 and D-4 profiles. The second area of greater thickness was discovered in the eastern part of the dome (Fig. 4b). The glacier ice along the subglacial step is ~50–75 m thick.

The mean thickness of WG is greater than on DD, 99.6 ± 1.8 m compared with 32.4 ± 1.2 m. The greatest thickness was observed in the central part of this valley glacier, where the glacier ice was as much as 158 ± 2 m thick. The ice thickness of WG decreases towards the eastern glacier margin, which abuts a steep valley side. In contrast with the eastern margin, greater thickness values (63–125 m) were recorded along the western margin of WG (Fig. 5b). The basal reflection remains well below the lateral moraine surface, indicating that glacier ice extends beyond the current visible glacier limit.

The volume of DD decreased from 0.23 ± 0.03 km^3 to 0.16 ± 0.02 km^3 between 1979 and 2006. The glacier lost 30.4% of its volume at a mean annual rate of 0.003 ± 0.002 km^3 a^{-1}. For WG, the values of the total volume changed from 0.27 ± 0.02 km^3 to 0.24 ± 0.01 km^3. The volume loss was 10.6% and the mean annual change was 0.001 ± 0.001 km^3 a^{-1} over the period 1979–2006. The volume change calculated for the dome was almost three times as high as for the valley glacier.

INTERPRETATION AND DISCUSSION
Spatial variability in bed topography and surface lowering

The strong reflection observed in the GPR data from the flat-bottomed part of DD is interpreted as the transition from glacier ice to solid bedrock. A possible interpretation of weaker reflectors in the eastern flank of the plateau is that sediments rather than solid bedrock form the glacier bed in this area. A channel-like depression incised in the southeast subglacial margin of the plateau suggests that the bedrock has been deepened and widened by glacial erosion of an outlet glacier (Figs 2a and 4a). The incised terrain in the northeast margin of the plateau (Fig. 4a) indicates that
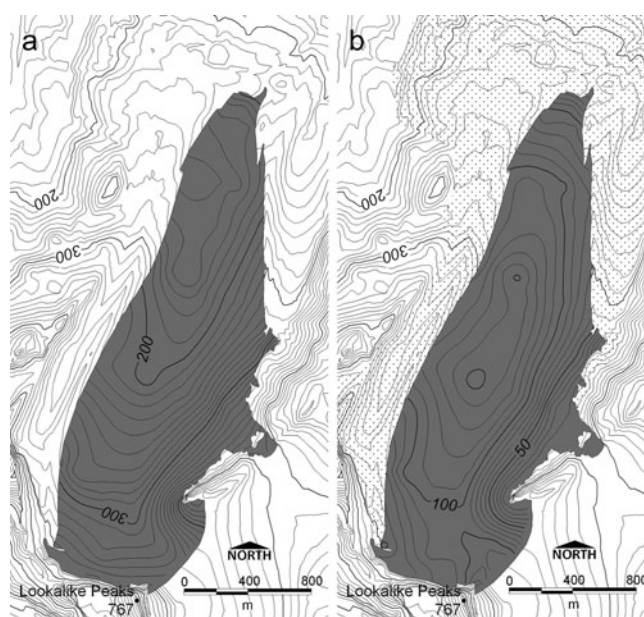

Fig. 5. (a) Bed topography and (b) ice thickness at WG based on the 2006 DEM and GPR measurements. The investigated valley glacier is marked in dark grey, and the maximum possible extent of debris-cored glacier area is shown by dots.

another outlet glacier has probably at some time in the past drained the northeastern part of DD towards the Abernethy Flats. The timing of this outlet glacier advance is unresolved by our data, but it might have been synchronous with a mid-Holocene advance of WG (Rabassa and others, 1982) dated by Hjort and others (1997) at ~4600 ^{14}C BP. The interpolated flatter subglacial relief in the northern part of DD (Fig. 4a) leads us to suggest that DD has not expanded to inundate cirques on the northern margin of the DD mesa. The fact that the steep cirque headwalls have sharp upper edges is also evidence that these rock lips have not been subjected to basal glacier erosion. This contrasts with the southeastern edge of the DD mesa beneath the outlet flowing towards Whisky Bay.

The strong reflection beneath the upper reaches of WG and the straight long profile of the bed suggest that the bed there is solid rock. By contrast, in the lower part of the glacier the reflection from the assumed glacier bed is weak, tentatively indicating a transition from ice to subglacial till. Thick ice at the western periphery of WG and debris-covered ice in adjacent moraine ridges together suggest that WG is more extensive than the present bare-ice surface would otherwise suggest. A large ice thickness along the western margin of the snout supports the hypothesis that a

Table 3. Changes of surface area, elevation and volume of DD and WG between 1979 and 2006

|	1979	2006	Change	Mean annual change
Davies Dome (without outlet)				
Mean elevation (m a.s.l.)	377.0 ± 2.0	368.5 ± 0.8	-8.5 ± 2.8 (−2.3%)	-0.32 ± 0.10 (−0.1%)
Surface area (km^2)	6.23 ± 0.05	4.94 ± 0.01	-1.29 ± 0.06 (−20.7%)	-0.048 ± 0.002 (−0.8%)
Volume (km^3)	0.23 ± 0.03	0.16 ± 0.02	-0.07 ± 0.05 (−30.4%)	-0.003 ± 0.002 (−1.1%)
Whisky Glacier				
Mean elevation (m a.s.l.)	350.7 ± 2.0	340.6 ± 0.8	-10.1 ± 2.8 (−2.9%)	-0.37 ± 0.10 (−0.1%)
Surface area (km^2)	2.69 ± 0.02	2.40 ± 0.01	-0.28 ± 0.03 (−10.6%)	-0.011 ± 0.001 (−0.4%)
Volume (km^3)	0.27 ± 0.02	0.24 ± 0.01	-0.03 ± 0.03 (−10.6%)	-0.001 ± 0.001 (−0.4%)
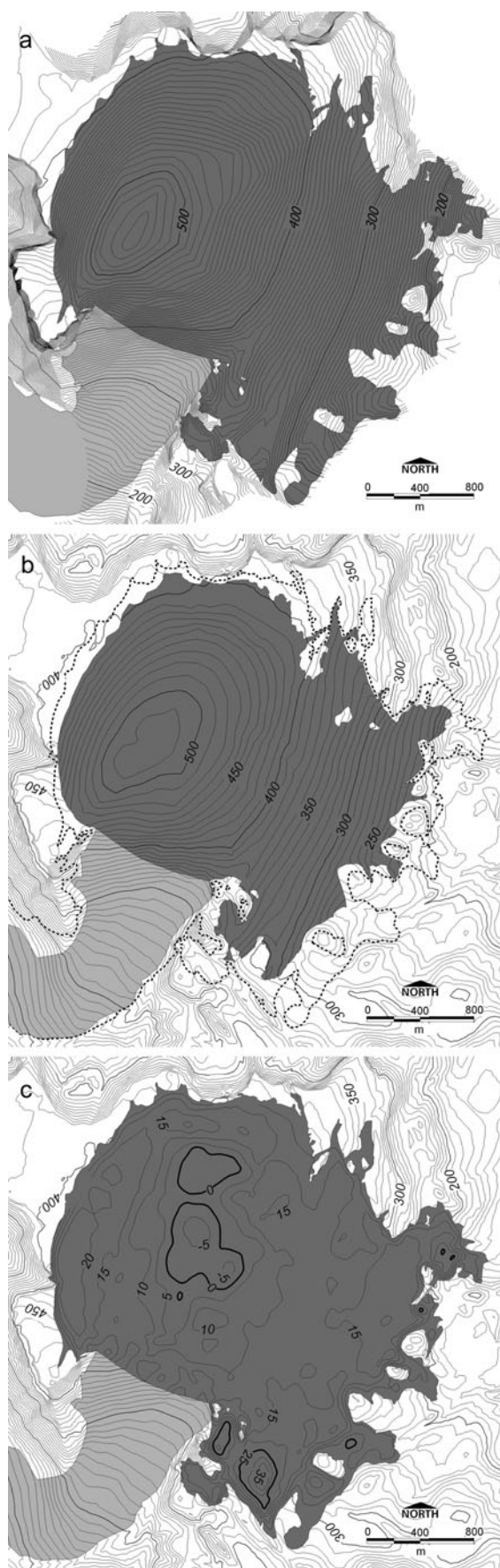
Fig. 6. Surface topography and elevation change at DD. Surface topography in (a) 1979 and (b) 2006 and (c) surface lowering between 1979 and 2006. The investigated dome glacier is marked in dark grey, the outlet glacier is shown in medium grey and the dotted line represents the 1979 ice outline (b). Isolines within the investigated glacier area in (c) represent surface change.

broad zone of the lateral moraine is an internal debris-covered part of WG (Chinn and Dillon, 1987).

The spatial distribution of surface lowering indicates that the two glaciers are evolving differently. At DD, ice surface reduced mainly at lower altitudes, while the accumulation zone experienced little or slightly positive change. By contrast, the whole surface area of WG experienced lowering, with the greatest magnitude in the upper reaches of the glacier. The local differences in surface lowering probably result from higher air temperatures on WG and from different flow patterns and surface mass balances of the two glaciers. The assumption of the different flow rate is consistent with ice velocities observed at mass-balance measurement sites on the two glaciers. The surface velocities on WG were nearly twice as high as on DD during the period 2009–11 (Nývlt and others, 2012). As the ice flow in the flat-bottomed upper part of DD is limited, the increased melting in lower parts of the dome was not compensated by transport of ice mass between the upper and lower parts of the glacier. By contrast, WG is a well-delimited valley glacier with high flow velocities (Nývlt and others, 2012) and the spatial distribution of ice volume is controlled by enhanced transport of ice mass. The higher total volume change calculated for DD probably results from lesser thickness of its margins and from the position of the dome, which is more exposed to air masses than is WG.

Comparison to other studies in the AP region

Although the AP ice sheet, island ice caps and valley glaciers cover ~80% of the AP region (Rau and Braun, 2002), volumetric characteristics are known only for a minority of glaciers (e.g. Davies and others, 2011). Apart from the AP ice sheet, data on ice thickness have been collected only on Alexander Island (Wager, 1982), Adelaide Island (Rivera and others, 2005), Anvers Island (Dewart, 1971), the South Shetland Islands (e.g. Macheret and others, 2009; Navarro and others, 2009), JRI (Rabassa and others, 1982) and Dolleman Island (Peel and others, 1988). At JRI, until recently the ice thickness was known only for Mount Haddington ice cap. According to radio-echo sounding, the ice dome is estimated to be ~300 m thick (Aristarain, 1980). This is a typical value for island ice caps along the AP as shown in Table 4. On DD the maximum ice thickness of ~83 m is about three times thinner than Mount Haddington, which is not unexpected given the smaller surface area of the dome compared with the extent of the JRI ice cap (587 km^2). The ice thickness of WG is similar to the thickness of Spartan Glacier at Alexander Island, which is the only valley glacier in the AP region with known thickness (Wager, 1982).

Areal changes observed on DD and WG confirm that the glacier retreat on JRI has increased in recent decades. According to Rau and others (2004), ice masses on JRI lost 3.9% in area during the period 1975–2002 and, of these, land-terminating glaciers were subject to the smallest retreat rates. By contrast, we find that the DD glacier area decreased by 22.1% and WG by 10.6% over the period 1979–2006. These values are in agreement with retreat rates of DD reported by Davies and others (2011) for the period 1988–2009. The difference in retreat rate of the two glaciers may be attributed to the faster downwasting of DD. The tidewater front of the DD outlet in Whisky Bay shows more prominent changes than the grounded glacier tongue of WG. During the last 30 years the surface area of DD and WG decreased at a mean rate of 0.8% a^{-1} and 0.4% a^{-1},
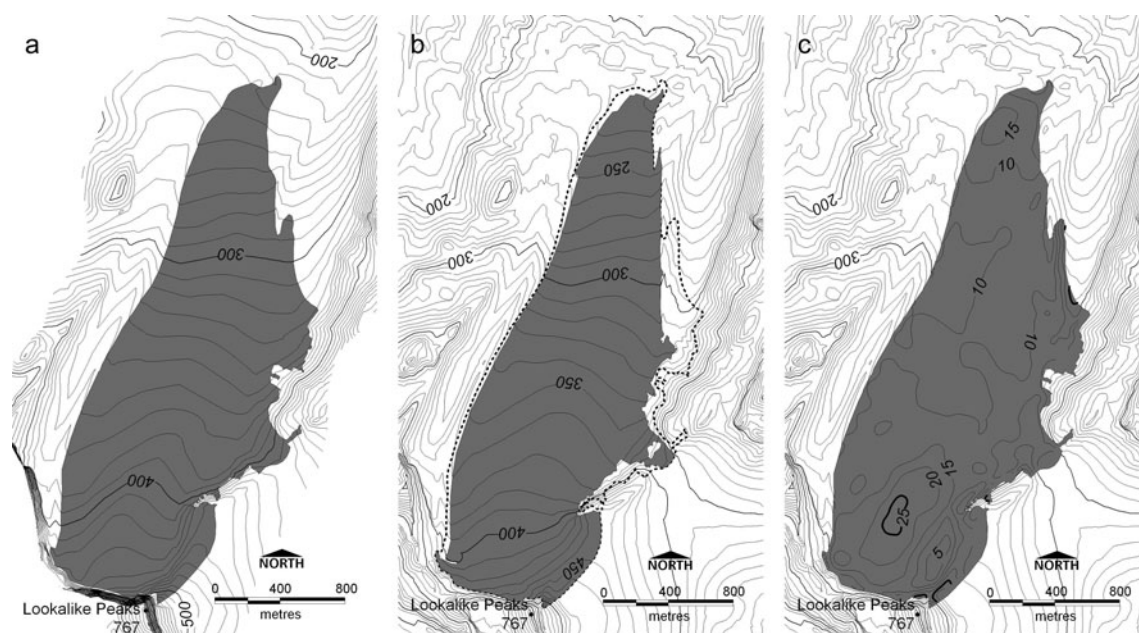
Fig. 7. Surface topography and elevation change at WG. Surface topography in (a) 1979 and (b) 2006 and (c) surface lowering between 1979 and 2006. The investigated valley glacier is marked in dark grey, and the dotted line represents the 1979 ice outline (b). Isolines within the investigated glacier area in (c) represent surface change.

respectively. These values are higher than mean annual areal changes of ice caps on Livingston Island (Calvet and others, 1999; Molina and others, 2007) and King George Island (Simões and others, 1999) over the period 1956–2000 (Table 5). By contrast, the mean annual area decrease of DD and WG is an order of magnitude less than the mean annual area loss of cirque glaciers on King George Island (Simões and others, 2004). Overall, the increase in glacier retreat observed on JRI is similar to the accelerated area loss reported for glaciers on King George Island in the period 2000–08 (Rückamp and others, 2011).

The mean elevations of DD and WG decreased by 0.3 ± 0.1 and $0.4 \pm 0.1 \, \mathrm{m \, a^{-1}}$, respectively. These values

correspond well with the mean surface lowering of 0.32 m w.e. $\mathrm{a^{-1}}$ observed over the period 1988–97 at Rothera Point on the southwestern AP (Smith and others, 1998) and with the mean lowering rate of $0.2 \, \mathrm{m \, a^{-1}}$ reported from the summit of Bellingshausen Dome on King George Island (Rückamp and others, 2011). By contrast, our estimates are lower than values reported from Vega Island, Livingston Island and the eastern part of King George Island. According to recent observations on Vega Island (Skvarca and De Angelis, 2003; Skvarca and others, 2004), mean annual surface lowering of Glaciar Bahía del Diablo ranged from 1.0 to $1.6 \, \mathrm{m \, a^{-1}}$ over the period 1985–2003. Pritchard and others (2009) and Rückamp and others (2011) reported a

Table 4. Comparison of the maximum ice thickness of island glaciers along the Antarctic Peninsula

Island	Glacier		Maximum thickness	Method	Source
	Name	Type*	m		
Adelaide	Fuchs Ice Piedmont	P	300	RES	Rivera and others (2005)
Alexander	Spartan Glacier	V	220	RES	Wager (1982)
Anvers	Anvers	IC	600	Gravimetry	Dewart (1971)
Dolleman	Dolleman	IC	460	?	Peel and others (1988)
James Ross	Mount Haddington	IC	300	RES	Rabassa and others (1982)
	Davies Dome	IC	83	GPR	This study
	Whisky Glacier	V	157	GPR	This study
King George	King George	IC	395	RES	Pfender (1999)
	Lange Glacier	O	308	RES	Macheret and Moskalevsky (1999)
	Fourcade Glacier	IC	79	GPR	Kim and others (2010)
	Bellingshausen Dome	IC	120	GPR	Sobiech (2009)
Livingston	Livingston ice cap	IC	200	RES	Macheret and others (2009)
	Bowles Plateau	IC	500	RES	Macheret and others (2009)
	Johnsons Glacier	TW	196	RES	Macheret and others (2009)
	Hurd Glacier	IC	205	RES	Macheret and others (2009)
Nelson	Nelson	IC	169	RES	Ren and others (1995)

*IC: ice cap; V: valley; O: outlet; P: piedmont; TW: tidewater.

Table 5. Mean annual area changes of island glaciers along the northern part of the Antarctic Peninsula

Island	Glacier		Period	Mean area change		Source
	Name	Type*		$km^2 a^{-1}$	%	
James Ross	39 glaciers		1975–88	1.84	0.1	Skvarca and others (1995)
			1988–93	2.08	0.1	
	58 glaciers		1988–2001	3.79	0.2	Rau and others (2004)
	Davies Dome	IC	1979–2006	0.048	0.8	This study
	Whisky Glacier	V	1979–2006	0.011	0.4	This study
Livingston	Hurd Glacier	IC	1956–2000	0.0116	0.2	Molina and others (2007)
	Johnsons Glacier	TW	1956–2000	0.0002	0.004	Molina and others (2007)
	Livingston ice cap	IC	1956–96	0.7902	0.1	Calvet and others (1999)
King George	King George Island	IF	1956–95	2.28	0.2	Simões and others (1999)
	ice field		2000–08	2.56	0.2	Rückamp and others (2011)
	Babylon Glacier	H	1979–2000	0.0046	2.7	Simões and others (2004)
	Ferguson Glacier	C	1979–2001	0.0078	4.0	Simões and others (2004)
	Flagstaff Glacier	C	1979–2002	0.0053	3.1	Simões and others (2004)
	Lange Glacier	O	1956–2000	0.0455	0.2	Barboza and others (2004)
	Noble Glacier	V	1979–2003	0.0049	2.1	Simões and others (2004)
	Stenhouse Glacier	IC	1956–2000	0.0100	0.1	Simões and others (2004)

*C: cirque; H: hanging; IC: ice cap; IF: ice field; V: valley; O: outlet; TW: tidewater.

similar value of ~1.5 m a^{-1} on the South Shetland Islands for the periods 2003–07 and 2000–08, respectively. Ximenis and others (1999) obtained even higher lowering rates (1–5 m a^{-1}) for glaciers on Livingston Island during the period 1995–97. Comparison of the 1979 and 2006 DEMs revealed a mean annual volume loss of 1.1% a^{-1} at DD and 0.4% a^{-1} at WG. The value for WG corresponds with mean annual glacier volume loss (0.2–0.3% a^{-1}) reported for the South Shetland Islands for the period 1956–2000 (Molina and others, 2007). The value obtained at DD is three to four times higher than the mean annual volume loss of Hurd (0.3% a^{-1}) and Johnsons Glaciers (0.2% a^{-1}) according to volume change described by Molina and others (2007).

A comparison of our spatial data with earlier glaciological observations suggests that DD and WG were subject to greater retreat, surface lowering and ice volume loss than other island ice caps in the AP region. If the recent rate of volume loss continues, DD and WG could disappear within 62 ± 52 and 227 ± 220 years, respectively. This approximated timing corresponds well with the value based on mean rate of areal loss for WG (228 ± 22 years to extinction), but the volumetric change of DD is more rapid than its areal change (104 ± 5 years). However, we assume that area rather than volume has the largest control on the future development of both glaciers. The estimated melting time of WG based on both areal and volumetric changes is consistent with the estimated future evolution of Bellingshausen Dome on King George Island, which is predicted to completely disappear after 285 years if the present warming trend persists (Rückamp and others, 2011). A total disappearance of cirque glaciers will probably occur much faster, as was shown by Simões and others (2004) for Ferguson and Flagstaff Glaciers on King George Island.

SUMMARY AND CONCLUDING REMARKS

GPR data acquired in 2010 indicate that the subglacial topography of an ice dome and of a valley glacier in the northern part of JRI differ significantly. A near-flat plateau forms the glacier bed of the upper accumulation area of DD, whereas a steep plateau edge and dissected topography underlie the lower elevated eastern part of the dome. In contrast, almost uniform glacier bed topography exists beneath WG. The maximum ice thicknesses as measured by GPR at DD and WG are 83 ± 2 and 158 ± 2 m, respectively. The average surface elevation of the dome decreased by 8.5 ± 2.8 m between 1979 and 2006, whereas the valley glacier experienced average surface lowering of 10.1 ± 2.8 m. DD lost 22.1% of its area between 1979 and 2006, decreasing from 8.33 ± 0.06 km^2 to 6.49 ± 0.01 km^2. A dome area of the glacier decreased from 6.23 ± 0.05 km^2 to 4.94 ± 0.01 km^2 (–20.7%) and its volume changed from 0.26 ± 0.03 km^3 to 0.16 ± 0.02 km^3 (–30.4%). The surface area of WG decreased from 2.69 ± 0.02 km^2 to 2.40 ± 0.01 km^2 (–10.6%), resulting in the glacier mass loss from 0.27 ± 0.02 km^3 to 0.24 ± 0.01 km^3 (–10.6%). Between 1979 and 2006, glacial area loss ranged from an average of 0.048 ± 0.002 km^2 a^{-1} (DD) to 0.011 ± 0.001 km^2 a^{-1} (WG). Average volume losses of DD and WG were 0.003 ± 0.001 and 0.001 ± 0.001 km^3 a^{-1}, respectively. The observed changes are higher than areal and volumetric losses reported from the AP region between 62° and 68° S. If the recent trend in air temperature continues, DD and WG may disappear in 104 ± 5 and 228 ± 22 years, respectively. However, model projections reported by Carril and others (2005) show that an increase in temperature trends is expected over the 21st century.

REFERENCES

Aristarain AJ (1980) *Étude glaciologique de la calotte polaire de l'île James Ross (Péninsule Antarctique).* Université Grenoble, Grenoble (Centre National de la Recherche Scientifique Publication 322)

Barboza HHC, de Bortoli ÁL, Simões JC, da Cunha RD and Braun M (2004) Bidimensional numerical simulation of the Lange Glacier, King George Island, Antarctica: preliminary results. *Pesqui. Antárt. Brasil.,* **4**, 67–76

British Antarctic Survey (2010) *Northern Antarctic Peninsula, 1:250 000 scale. Map No. BAS/UKAH, Sheet 3.* British Antarctic Survey, Cambridge

Calvet J, García-Sellés D and Corbera J (1999) Fluctuaciones de la extensión del casquete glacial de la Isla Livingston (Shetland del Sur) desde 1956 hasta 1996. *Acta Geol. Hispán.,* **34**(4), 365–374

Carril AF, Menéndez CG and Navarra A (2005) Climate response associated with the Southern Annular Mode in the surroundings of Antarctic Peninsula: a multimodel ensemble analysis. *Geophys. Res. Lett.,* **32**(16), L16713 (doi: 10.1029/2005GL023581)

Chinn TJH and Dillon A (1987) Observations on a debris-covered polar glacier 'Whisky Glacier', James Ross Island, Antarctic Peninsula, Antarctica. *J. Glaciol.,* **33**(115), 300–310

Cook AJ, Fox AJ, Vaughan DG and Ferrigno JG (2005) Retreating glacier fronts on the Antarctic Peninsula over the past half-century. *Science,* **308**(5721), 541–544 (doi: 10.1126/science.1104235)

Czech Geological Survey (2009) *James Ross Island – northern part.* Czech Geological Survey, Praha

Davies BJ, Carrivick JL, Glasser NF, Hambrey MJ and Smellie JL (2011) A new glacier inventory for 2009 reveals spatial and temporal variability in glacier response to atmospheric warming in the Northern Antarctic Peninsula, 1988–2009. *Cryos. Discuss.,* **5**(6), 3541–3595 (doi: 10.5194/tcd-5-3541-2011)

Dewart G (1971) Gravimeter observations on Anvers Island and vicinity. In Crary AP ed. *Antarctic snow and ice studies II.* American Geophysical Union, Washington, DC, 179–190 (Antarctic Research Series 16)

Fountain AG, Lewis KJ and Doran PT (1999) Spatial climatic variation and its control on glacier equilibrium line altitude in Taylor Valley, Antarctica. *Global Planet. Change,* **22**(1–4), 1–10

Garmin International (2009) *GPSMAP 60CSx with sensors and maps: owner's manual.* Garmin International Inc., Olathe, KS. http://aspdf.com/ebook/gpsmap-60csx-with-sensors-and-maps-owner's-manual-pdf.html (accessed 27 April 2012)

Glasser NF, Scambos TA, Bohlander J, Truffer M, Pettit EC and Davies BJ (2011) From ice-shelf tributary to tidewater glacier: continued rapid recession, acceleration and thinning of Röhss Glacier following the 1995 collapse of the Prince Gustav Ice Shelf, Antarctic Peninsula. *J. Glaciol.,* **57**(203), 397–406 (doi: 10.3189/002214311796905578)

Gudmundsson GH and Bauder A (1999) Towards an indirect determination of the mass-balance distribution of glaciers using the kinematic boundary condition. *Geogr. Ann.,* **81A**(4), 575–583

Hjort C, Ingólfsson Ó, Möller P and Lirio JM (1997) Holocene glacial history and sea level changes on James Ross Island, Antarctic Peninsula. *J. Quat. Sci.,* **12**(4), 259–273

Ingólfsson Ó, Hjort C, Björck S and Smith RIL (1992) Late Pleistocene and Holocene glacial history of James Ross Island, Antarctic Peninsula. *Boreas,* **21**(3), 209–222

Jol HM (2009) *Ground penetrating radar theory and applications.* Elsevier Science, Amsterdam

Kim KY, Lee J, Hong MH, Hong JK and Shon H (2010) Helicopter-borne and ground-towed radar surveys of the Fourcade Glacier on King George Island, Antarctica. *Expl. Geophys.,* **41**(1), 51–60 (doi: 10.1071/EG09052)

King JC (1994) Recent climate variability in the vicinity of the Antarctic Peninsula. *Int. J. Climatol.,* **14**(4), 357–369

King JC, Turner J, Marshall GJ, Connolley WM and Lachlan-Cope TA (2003) Antarctic Peninsula climate variability and its causes as revealed by analysis of instrumental records. In Domack EW, Burnett A, Leventer A, Conley P, Kirby M and Bindschadler R eds. *Antarctic Peninsula climate variability: a historical and paleoenvironmental perspective.* American Geophysical Union, Washington, DC, 17–30 (Antarctic Research Series 79)

Knap WH, Oerlemans J and Cadée M (1996) Climate sensitivity of the ice cap of King George Island, South Shetland Islands, Antarctica. *Ann. Glaciol.,* **23**, 154–159

Kovacs A, Gow AJ and Morey RM (1995) The in-situ dielectric constant of polar firn revisited. *Cold Reg. Sci. Technol.,* **23**(3), 245–256

Láska K, Budík L, Budiková M and Prošek P (2011) Method of estimating solar UV radiation in high-latitude locations based on satellite ozone retrieval with an improved algorithm. *Int. J. Remote Sens.,* **32**(11), 3165–3177 (doi: 10.1080/01431161.2010.541513)

Láska K, Nývlt D, Engel Z and Budík L (2012) Seasonal variation of meteorological variables and recent surface ablation/accumulation rates on Davies Dome and Whisky Glacier, James Ross Island, Antarctica. *Geophys. Res. Abstr.,* **14** (EGU2012-5545)

Macheret YuYa and Moskalevsky MYu (1999) Study of Lange Glacier on King George Island, Antarctica. *Ann. Glaciol.,* **29**, 202–206 (doi: 10.3189/172756499781820941)

Macheret YuYa and 6 others (2009) Ice thickness, internal structure and subglacial topography of Bowles Plateau ice cap and the main ice divides of Livingston Island, Antarctica, by ground-based radio-echo sounding. *Ann. Glaciol.,* **50**(51), 49–56 (doi: 10.3189/172756409789097478)

MALÅ GeoScience (2005) *Ramac GPR. Hardware manual.* MALÅ GeoScience, Malå

Marshall GJ (2002) Analysis of recent circulation and thermal advection change in the northern Antarctic Peninsula. *Int. J. Climatol.,* **22**(12), 1557–1567 (doi: 10.1002/joc.814)

Marshall GJ, Orr A and Van Lipzig NPM (2006) The impact of a changing Southern Hemisphere annular mode on Antarctic Peninsula summer temperatures. *J. Climate,* **19**(20), 5388–5404

Meixner P (2009) Mapping in Antarctica. *GEODIS News* 8, 8–9 http://www.geodis.cz/uploads/dokumenty/pdf_casopis/GEODIS_NEWS_english_2009.pdf (accessed 27 April 2012)

Molina C, Navarro FJ, Calver J, García-Sellés D and Lapazaran JJ (2007) Hurd Peninsula glaciers, Livingston Island, Antarctica, as indicators of regional warming: ice-volume changes during the period 1956–2000. *Ann. Glaciol.,* **46**, 43–49 (doi: 10.3189/172756407782871765)

Narod BB and Clarke GKC (1994) Miniature high-power impulse transmitter for radio-echo sounding. *J. Glaciol.,* **40**(134), 190–194

Navarro FJ and Eisen O (2010) Ground-penetrating radar in glaciological applications. In Pellikka P and Reese WG eds. *Remote sensing of glaciers: techniques for topographic, spatial and thematic mapping of glaciers.* Taylor & Francis, London, 195–229

Navarro FJ and 6 others (2009) Radioglaciological studies on Hurd Peninsula glaciers, Livingston Island, Antarctica. *Ann. Glaciol.,* **50**(51), 17–24 (doi: 10.3189/172756409789097603)

Nývlt D, Kopačková V, Láska K and Engel Z (2010) Recent changes detected on two glaciers at the northern part of James Ross Island, Antarctica. *Geophys. Res. Abstr.,* **12** (EGU2010-8102)

Nývlt D and 6 others (2012) Glacial history of James Ross Island since the Late Glacial. In Blahůt J, Klimeš J, Stěpančiková P and Hartvich F eds *Geomofologický sborník 10.* Ústav struktury a mechaniky hornin, Praha, 35–36

Paterson WSB (1994) *The physics of glaciers,* 3rd edn. Elsevier, Oxford

Peel DA, Mulvaney R and Davison BM (1988) Stable-isotope/air-temperature relationships in ice cores from Dolleman Island and the Palmer Land plateau, Antarctic Peninsula. *Ann. Glaciol.,* **10**, 130–136

Pellikka P and Rees WG (2009) *Remote sensing of glaciers: techniques for topographic, spatial and thematic mapping of glaciers*. Taylor and Francis, London

Pfender M (1999) Topographie und Glazialhydrologie von King George Island, Antarktis. (Master's thesis, Westfälische Wilhelms-Universität Münster)

Plewes LA and Hubbard B (2001) A review of the use of radio-echo sounding in glaciology. *Progr. Phys. Geogr.,* **25**(2), 203–236 (doi: 10.1177/030913330102500203)

Pritchard HD, Arthern RJ, Vaughan DG and Edwards LA (2009) Extensive dynamic thinning on the margins of the Greenland and Antarctic ice sheets. *Nature,* **461**(7266), 971–975 (doi: 10.1038/nature08471)

Rabassa J (1983) Stratigraphy of the glacigenic deposits in northern James Ross Island, Antarctic Peninsula. In Evenson EB, Schlüchter C and Rabassa J eds. *Tills and related deposits: genesis/petrology/ application/stratigraphy*. A.A. Balkema, Rotterdam, 329–340

Rabassa J, Skvarca P, Bertani L and Mazzoni E (1982) Glacier inventory of James Ross and Vega Islands, Antarctic Peninsula. *Ann. Glaciol.,* **3**, 260–264

Rau F and Braun M (2002) The regional distribution of the dry-snow zone on the Antarctic Peninsula north of 70° S. *Ann. Glaciol.,* **34**, 95–100 (doi: 10.3189/172756402781817914)

Rau F and 8 others (2004) Variations of glacier frontal positions on the northern Antarctic Peninsula. *Ann. Glaciol.,* **39**, 525–530 (doi: 10.3189/172756404781814212)

Ren J and 8 others (1995) Glaciological studies on Nelson Island, South Shetland Islands, Antarctica. *J. Glaciol.,* **41**(138), 408–412

Rignot E and 6 others (2008) Recent Antarctic ice mass loss from radar interferometry and regional climate modelling. *Nature Geosci.,* **1**(2), 106–110 (doi: 10.1038/ngeo102)

Rippin D, Vaughan DG and Corr HFJ (2011a) The basal roughness of Pine Island Glacier, West Antarctica. *J. Glaciol.,* **57**(201), 67–76 (doi: 10.3189/002214311795306574)

Rippin DM, Carrivick JL and Williams C (2011b) Evidence towards a thermal lag in the response of Kårsaglaciären, northern Sweden, to climate change. *J. Glaciol.,* **57**(205), 895–903 (doi: 10.3189/002214311798043672)

Rivera A and 7 others (2005) Glacier wastage on southern Adelaide Island, Antarctica, and its impact on snow runway operations. *Ann. Glaciol.,* **41**, 57–62 (doi: 10.3189/172756405781813401)

Rückamp M, Braun M, Suckro S and Blindow N (2011) Observed glacial changes on the King George Island ice cap, Antarctica, in the last decade. *Global Planet. Change,* **79**(1–2), 99–109 (doi: 10.1016/j.gloplacha.2011.06.009)

Sandmeier KJ (2008) *REFLEXW: processing program for seismic, acoustic and electromagnetic reflection, refraction and transmission data, Version 5.0.* Sandmeier Scientific Software, Karlsruhe

Simões JC, Bremer UF, Aquino FE and Ferron FA (1999) Morphology and variations of glacial drainage basins in the King George Island ice field, Antarctica. *Ann. Glaciol.,* **29**, 220–224 (doi: 10.3189/172756499781821085)

Simões JC, Dani N, Bremer UF, Aquino FE and Arigony-Neto J (2004) Small cirque glaciers retreat on Keller Peninsula, Admiralty Bay, King George Island, Antarctica. *Pesqui. Antárt. Brasil.,* **4**, 49–56

Skvarca P and De Angelis H (2003) Impact assessment of regional climate warming on glaciers and ice shelves of the northeastern Antarctic Peninsula. In Domack EW, Burnett A, Leventer A, Conley P, Kirby M and Bindschadler R eds. *Antarctic Peninsula climate variability: a historical and paleoenvironmental perspective*. American Geophysical Union, Washington, DC, 69–78 (Antarctic Research Series 79)

Skvarca P, Rott H and Nagler T (1995) Satellite imagery, a baseline for glacier variation study on James Ross Island, Antarctica. *Ann. Glaciol.,* **21**, 291–296

Skvarca P, Rack W, Rott H and Donángelo T (1998) Evidence of recent climatic warming on the eastern Antarctic Peninsula. *Ann. Glaciol.,* **27**, 628–632

Skvarca P, De Angelis H and Ermolin E (2004) Mass balance of 'Glaciar Bahía del Diablo', Vega Island, Antarctic Peninsula. *Ann. Glaciol.,* **39**, 209–213 (doi: 10.3189/ 172756404781814672)

Smith AM, Vaughan DG, Doake CSM and Johnson AC (1998) Surface lowering of the ice ramp at Rothera Point, Antarctic Peninsula, in response to regional climate change. *Ann. Glaciol.,* **27**, 113–118

Sobiech J (2009) Geometry and glacial hydrology of Bellingshausen Dome, King George Island, Antarctica: results from GPR-measurement. (Diploma thesis, Westfälische Wilhelms-Universität Münster)

Turner J and 8 others (2005) Antarctic climate change during the last 50 years. *Int. J. Climatol.,* **25**, 279–294

Vaughan DG, Marshall GJ, Connolley WM, King JC and Mulvaney R (2001) Climate change: devil in the detail. *Science,* **293**(5536), 1777–1779 (doi: 10.1126/science.1065116)

Vaughan DG and 8 others (2003) Recent rapid regional climate warming on the Antarctic Peninsula. *Climatic Change,* **60**(3), 243–274

Wager AC (1982) Mapping the depth of a valley glacier by radio-echo sounding. *Br. Antarct. Surv. Bull.* 51, 111–123

Ximenis L, Calvet J, Enrique J, Corbera J, de Gamboa CF and Furdada G (1999) The measurement of ice velocity, mass balance and thinning-rate on Johnsons Glacier, Livingston Island, South Shetland Islands, Antarctica. *Acta Geol. Hispán.,* **34**(4), 403–409